PROGRESS IN THE OPERATIONALISATION OF THE TSA FOR THE COMPUTATION OF NON-LINEAR FOUR-WAVE INTERACTIONS IN DISCRETE SPECTRAL WAVE MODELS

Gerbrant van Vledder[1,2]

[1)]Alkyon Hydraulic Consultancy & Research
PO Box 248, 8300 AE Emmeloord, The Netherlands
vledder@alkyon.nl

[2)]Delft University of Technology,
P.O. Box, 5048, 2600 GA, Delft, The Netherlands
g.p.vanvledder@tudelft.nl

1 INTRODUCTION

This paper describes the progress made in the development of an operational Two Scale Approximation (TSA) for the computation of non-linear four-wave interactions in discrete wave spectra (Hasselmann, 1962). The first ideas of a two-scale method where already described by Resio et al. (1992). A formal framework of the TSA was presented by Resio and Perrie (2008). The TSA is a hybrid method using a combination of pre-computed exact non-linear transfer rates and correction terms. An attractive feature of the TSA is that it has the same mathematical structure for deep and shallow water.

Computations by Resio and Perrie (2008, 2009) show that the TSA is able to approximate the exact non-linear transfer rate rather well for a wide range of academic and measured spectra. These promising results suggest that the TSA qualifies for inclusion in operational discrete spectral wave prediction models. In this way an acceptable balance might be achieved between computational requirements and accuracy. A successful implementation of the TSA in operational wave models might replace the Discrete Interaction Approximation (DIA), which was developed by Hasselmann et al. (1985). This would be a welcome development since the DIA has some limitations that hamper the development of wave models (cf. Van Vledder et al., 2000). Initial steps towards the operationalisation of the TSA are described in Van Vledder (2007). This paper can be considered as a sequel to that paper. In this paper we pay attention to practical and operational aspects of the TSA and its limitations in view of its approximate nature. Other applications of the TSA are given in Long and Resio (2009).

The basic feature of the TSA is to split an arbitrary input spectrum in two parts. The first part is referred to as the broadband structure which captures the main shape of the input wave spectrum and which can be described parametrically, e.g. by a JONSWAP spectrum. The second part is the residual part, defined as the difference between the arbitrary input wave spectrum and the parametric spectrum. An example of such a

division of an arbitrary spectrum into a broad-band spectrum and its residue is given in Figure 1.

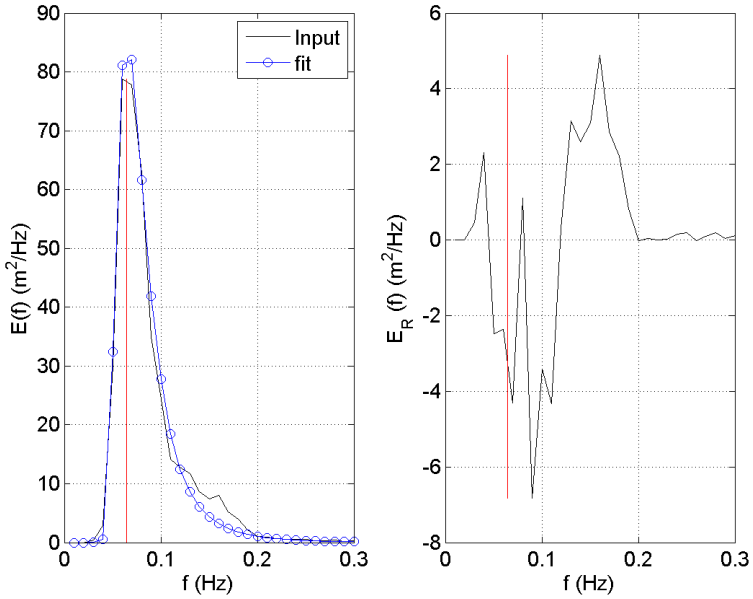

Figure 1: Example of the decomposition of arbitrary spectrum into a broad band spectrum (left panel) and its residual spectrum (right panel). The red vertical line denotes the position of the peak frequency.

The non-linear transfer rate of the total wave spectrum is computed in two steps. In the first step the non-linear transfer rate for the broadband spectrum is obtained from a database with pre-computed exact transfer rates, for instance with the WRT method (Van Vledder, 2006). This part of the solution is referred to as the **first** scale. Using a database implies that only a finite number of spectral shapes is included in the database. In the second step the total transfer rate is determined by adding the contribution of so-called cross terms. These consist of the residual spectral densities, pre-computed coupling coefficients and Jacobians. These cross terms can be considered as correction terms to the non-linear transfer rate of the broadband spectrum. This part of the solution is referred to as the **second** scale. Since not all cross terms are accounted for, some approximations are made in the TSA method.

The inclusion of the TSA in a discrete spectral wave model is of practical interest. To that end, the TSA should be written in subroutine form. The input of such a subroutine is the discrete wave spectrum in combination with the discrete frequencies (or wave numbers), discrete angles and the water depth. The output of the subroutine consists of the non-linear transfer rate. Optionally, additional input and output arguments can be specified in such a way that they control the inner workings of the TSA and report on possible problems in the evaluation of the TSA.

The operationalisation of the TSA comprises transforming the research version of the TSA code into a generally applicable subroutine that can be implemented in any third-generation spectral wave model, like STWAVE, SWAN, WAM and WAVEWATCH.

The structure of this paper is as follows. Section 2 describes the TSA method and its resemblance with the WRT method. The application of the TSA for an arbitrary spectrum is discussed in Chapter 3. Chapter 4 presents results of some sensitivity computations to assess the limitations of the TSA. In other words, when does the TSA break down? Finally, conclusions and an outlook for further investigations are given in Chapter 5.

2 DESCRIPTION OF THE TSA METHOD

The TSA method is based on the WRT-method for the computation of the non-linear transfer rate in a discrete wave spectrum (Tracy and Resio, 1982, Resio and Perrie, 1991). The WRT-method is based on Webb's (1978) choice of transformations to remove the δ-functions in the Boltzmann integral derived by Hasselmann (1962). Following Van Vledder (2006) the non-linear transfer rate or rate of change of the action density n_1 at wave number k_1 can be written as:

$$\frac{\partial n_1}{\partial t} = \iint k_3 dk_3 d\theta_3 T\left(\boldsymbol{k}_1, \boldsymbol{k}_3\right) \tag{1}$$

in which the transfer function T is given by:

$$\begin{aligned} T\left(\boldsymbol{k}_1, \boldsymbol{k}_3\right) = \iint d\boldsymbol{k}_2 d\boldsymbol{k}_4 \times G \times \delta\left(\boldsymbol{k}_1 + \boldsymbol{k}_2 - \boldsymbol{k}_3 - \boldsymbol{k}_4\right) \\ \times \delta\left(\omega_1 + \omega_2 - \omega_3 - \omega_4\right) \times \left[n_1 n_3 \left(n_4 - n_2\right) + n_2 n_4 \left(n_3 - n_1\right) \right] \end{aligned} \tag{2}$$

The term G is the coupling coefficient, which is a function of all four wave numbers involved in an interaction. The δ-functions reflect the resonance conditions, or equivalently, they ensure the conservation of energy, action and momentum. As described in Van Vledder (2006) removing the delta-functions in (1) leads to the following expression for the function T:

$$T\left(\boldsymbol{k}_1, \boldsymbol{k}_3\right) = \oint_s ds \times G \times J \times N_{1,2,3,4} \,. \tag{3}$$

The function T consists of a line integral over a closed locus in wave number space and where G, J and $N_{1,2,3,4}$ are functions of the locus coordinate s. The locus can be considered as the solution in wave number space of the resonance conditions for a given combination of the wave numbers $\boldsymbol{k}_1$ and $\boldsymbol{k}_3$. In (3) J is the Jacobian term given by:

$$J = \left| \boldsymbol{c}_{g,2} - \boldsymbol{c}_{g,4} \right|^{-1} \tag{4}$$

The term $N_{1,2,3,4}$ is the product term of action densities

$$N_{1,2,3,4} = n_1 n_3 \left(n_4 - n_2\right) + n_2 n_4 \left(n_3 - n_1\right) \tag{5}$$

Details about the determination of the locus and the evaluation of (3) can be found in Van Vledder (2006).

As noted before, the basic feature of the TSA method is to split the spectrum n into a broadband spectrum b and a perturbation spectrum p for all four wave numbers involved in an interaction according to:

$$n_i = b_i + p_i \quad \text{for} \quad i = 1,4 \tag{6}$$

Substitution of (6) into the product term of action densities $N_{1,2,3,4}$ leads to

$$\begin{aligned} N_{1,2,3,4} \;=\; & b_1 b_3 \left(b_4 - b_2\right) + b_2 b_4 \left(b_3 - b_1\right) + \\ & p_1 p_3 \left(p_4 - p_2\right) + p_2 p_4 \left(p_3 - p_1\right) + \\ & b_1 b_3 \left(p_4 - p_2\right) + b_2 b_4 \left(p_3 - p_1\right) + \\ & p_1 p_3 \left(b_4 - b_2\right) + p_2 p_4 \left(b_3 - b_1\right) + \\ & b_1 p_3 \left(b_4 - b_2\right) + b_2 p_4 \left(b_3 - b_1\right) + \\ & p_1 b_3 \left(b_4 - b_2\right) + p_2 b_4 \left(b_3 - b_1\right) + \\ & b_1 p_3 \left(p_4 - p_2\right) + b_2 p_4 \left(p_3 - p_1\right) + \\ & p_1 b_3 \left(p_4 - p_2\right) + p_2 b_4 \left(p_3 - p_1\right) \end{aligned} \tag{7}$$

The first line of Eq. (7) consists of action densities of the broadband spectrum. The second line contains action densities of the perturbation spectrum, whereas the other terms contain a varying mix of action densities from the broadband and perturbation spectrum. The complete transfer integral can be separated into the transfer rate of the broadband spectrum and seven additional contributions:

$$\frac{\partial n_1}{\partial t} = B\left(\boldsymbol{k}_1\right) + \sum\nolimits_{j=2}^{8} \iint \oint_s N_j G J \, ds \, k_3 \, d\theta_3 \, dk_3 \tag{8}$$

In (8) the subscript j refers to the j^{th} row in Eq. (8) and $B(\boldsymbol{k}_1)$ is the exact transfer rate for the broadband spectrum. Resio and Perrie (2007) argue that the terms in (7) containing the perturbation terms p_2 and p_4 can be omitted since they do not contribute significantly to the total transfer rate. A practical benefit of this assumption is that these terms are not easily known for a given decomposition of an arbitrary spectrum, whereas the other terms follow directly from the decomposition. Retaining the other terms yields

$$\begin{aligned} \tilde{N}_{1,2,3,4} \;=\; & b_1 b_3 \left(b_4 - b_2\right) + b_2 b_4 \left(b_3 - b_1\right) + \\ & b_2 b_4 \left(p_3 - p_1\right) + p_1 p_3 \left(b_4 - b_2\right) + \\ & b_1 p_3 \left(b_4 - b_2\right) + p_1 b_3 \left(b_4 - b_2\right) \end{aligned} \tag{9}$$

Substitution of (9) in Eq. (8) gives

$$\begin{aligned}\frac{\partial n_1}{\partial t} &= B(\boldsymbol{k}_1) + \iint \oint_s \left[b_2 b_4 (p_3 - p_1) + (p_1 p_3 + b_1 p_3 + p_1 b_3)(b_4 - b_2) \right] JG ds k_3 dk_3 d\theta_3 \\ &= B(\boldsymbol{k}_1) + \iint \left[(p_3 - p_1) \oint_s b_2 b_4 JG ds \right] k_3 dk_3 d\theta_3 \\ &\quad + \iint \left[(p_1 p_3 + b_1 p_3 + p_1 b_3) \oint_s (b_4 - b_2) JG ds \right] k_3 dk_3 d\theta_3 \end{aligned} \tag{10}$$

The terms $\oint_s b_2 b_4 JG ds$ and $\oint_s (b_4 - b_2) JG ds$ depend on the wave number combination $(\boldsymbol{k}_1, \boldsymbol{k}_3)$ but not on the actual action density terms. Therefore, they can be pre-computed. This is done using an adapted version of the WRT method. Following Resio and Perrie (2007) these terms can be written as a pumping term (product of the densities at the wave numbers $\boldsymbol{k}_1$ and $\boldsymbol{k}_3$) and a diffusive term (involving differences in densities of the wave numbers $\boldsymbol{k}_1$ and $\boldsymbol{k}_3$):

$$\begin{aligned}\Lambda_p(\boldsymbol{k}_1, \boldsymbol{k}_3) &= \oint_s (b_4 - b_2) JG ds \big|_{\boldsymbol{k}_1, \boldsymbol{k}_3} \\ \Lambda_d(\boldsymbol{k}_1, \boldsymbol{k}_3) &= \oint_s (b_2 b_4) JG ds \big|_{\boldsymbol{k}_1, \boldsymbol{k}_3} \end{aligned} \tag{11}$$

Combining the various equations leads to the following formulation of the TSA

$$\begin{aligned}\frac{\partial n_1}{\partial t} &= B(\boldsymbol{k}_1) + \iint (p_3 - p_1) \Lambda_d(\boldsymbol{k}_1, \boldsymbol{k}_3) k_3 dk_3 d\theta_3 \\ &\quad + \iint (p_1 p_3 + p_1 b_3 + b_1 p_3) \Lambda_p(\boldsymbol{k}_1, \boldsymbol{k}_3) k_3 dk_3 d\theta_3 \end{aligned} \tag{12}$$

Equation (12) reveals the formal structure of the TSA. Similar to the WRT method, this formulation is valid in deep and shallow water. For any given wave number $\boldsymbol{k}_1$ a loop over all spectral components $\boldsymbol{k}_3$ is to be made. The contributions to the transfer rate consist of products of action densities of the broadband spectrum and the perturbation spectrum, multiplied with tabulated data stored in the four-dimensional matrices Λ_d and Λ_p. The main difference with the WRT method is the absence of the repeated integration along the loci for each $\boldsymbol{k}_1$-$\boldsymbol{k}_3$ wave number combination, which saves a considerable amount time.

3 OPERATIONALISATION OF THE TSA

Discretisation

An important step in the operationalisation of the TSA is to discretise expression (12) such that it can be applied in a discrete spectral wave model. It is assumed that the wave spectrum is given in terms of a discrete energy density function of the discrete frequencies f_i (for i=1,N_f) and directions θ_j (j=1,N_θ) with a constant spacing $\Delta\theta$. An additional requirement is that the frequencies (or wave numbers) are distributed geometrically, viz. subsequent frequencies are related according to $f_{i+1}=(1+\delta) f_i$, with δ=0.1 typically. In practice, the proper Jacobian transformation between wave number space based action density spectra and frequency-direction energy density spectra must be applied since existing operational wave models use different conventions to represent and store discrete wave spectra. This may involve the basic variables (frequency f or radian frequency σ, or wave number k), of representing the spectrum in terms of variance (often denoted as energy) density E or action density $N=E/\sigma$, but also the order of the indices may be different, e.g E(f_i,θ_j) versus E(θ_i,f_j).

Based on expression (12) the non-linear transfer rate at a certain discrete wave number $\left(k_{i_{k1}},\theta_{j_{j1}}\right)$, and assuming a constant directional spacing $\Delta\theta$, is expressed as:

$$\begin{aligned}\Delta n\left(k_{i_{k1}},\theta_{j_{k1}}\right) = {} & B\left(k_{i_{k1}},\theta_{j_{k1}}\right) + \\ & + \sum_{i_{k3}=1}^{N_k}\sum_{j_{k3}}^{N_\theta}\left(p_{3i_{k3},j_{k3}} - p_{1i_{k3},j_{k3}}\right)\Lambda_d\left(i_{k1},j_{k1},i_{k3},j_{k3}\right)k_{i_{k3}}\Delta k_{i_{k3}}\Delta\theta \\ & + \sum_{i_{k3}=1}^{N_k}\sum_{j_{k3}}^{N_\theta}\left(p_{1i_{k1},j_{k1}}p_{3i_{k3},j_{k3}} + b_{1i_{k1},j_{k1}}p_{3i_{k3},j_{k3}} + p_{1i_{k1},j_{k1}}b_{3i_{k3},j_{k3}}\right)\Lambda_p\left(i_{k1},j_{k1},i_{k3},j_{k3}\right)k_{i_{k3}}\Delta k_{i_{k3}}\Delta\theta\end{aligned} \quad (13)$$

The above expression is the basic computational scheme of the TSA. Thus, for every spectral bin a loop is made over all spectral bins to compute the contribution of the cross terms using pre-computed data from the modified WRT method. In expression (13) the terms B, Λ_d and Λ_p are two- and four-dimensional matrices containing pre-computed results for a given broadband action density spectrum $b(\boldsymbol{k})$. These matrices are linked to each other since they are all based on the same broadband spectrum.

As with any approximate method the accuracy of the TSA degrades as the arbitrary spectrum deviates more and more from the broadband spectrum. A straightforward solution to this problem is to have a large but finite set of broadband spectra with associated pre-computed non-linear transfer rates and matrices Λ_d and Λ_p. These pre-defined spectra (and related transfer rate and matrices) must cover a wide range of spectral shapes regarding e.g. peak frequency, scale factor, peakedness and directional spreading to ensure accuracy of the TSA. It is therefore of interest to determine the number of required spectral shapes to enable the TSA to produce accurate answers. This question is considered in the next section.

4 LIMITATIONS OF THE TSA

Consistency check

To test the limitations of the TSA, a test program was carried out using spectra that slightly differ from a JONSWAP-type broad-band spectrum. The first test was a consistency test to check whether the TSA method gives the same answer as the WRT-method in the case that the perturbation spectrum is zero. Figure 2 shows a JONSWAP spectrum with a peak frequency of 0.2 Hz and a peak enhancement factor γ=2 and a directional spreading of 30° according to the $\cos^{2s}(\theta)$-model. In the right panel the non-linear transfer rate according to the WRT-method (X_{nl}), the DIA, and the TSA are shown. Since the perturbation spectrum is zero, the non-linear transfer rates according to the WRT-method, the broad-band transfer rate (X_{nl}^{BB}) and the rate according to the TSA method should be equal. As can be seen in Figure 2 this is indeed the case, showing that the generation and use of the pre-computed matrices Λ_d and Λ_p is correctly handled. Figure 2 also shows the typical signature of the DIA in comparison with an exact method for computing the non-linear transfer rate; a broader low-frequency positive lobe and a too deep negative lobe.

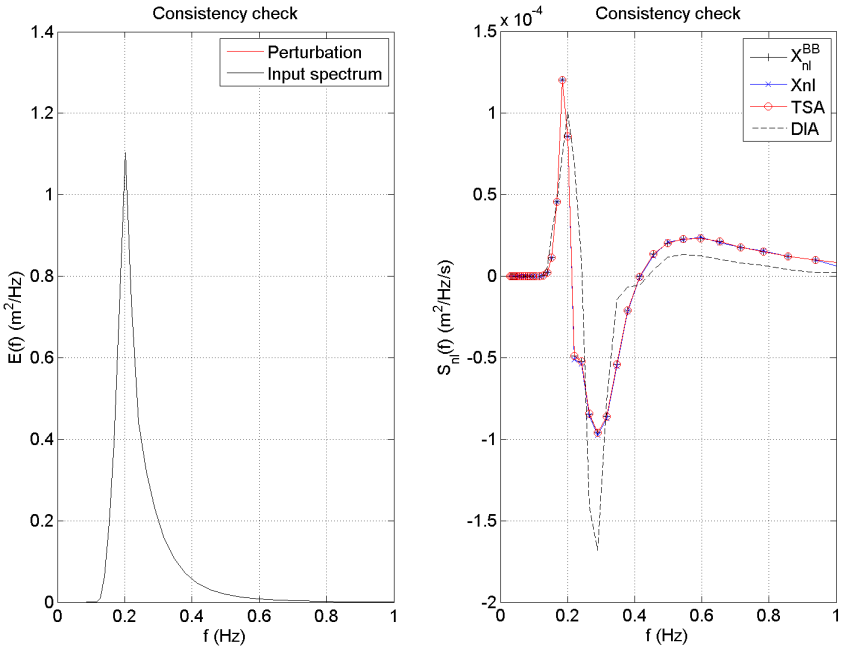

Figure 2: JONSWAP spectrum with f_p=0.2 Hz, γ=2 (left panel). Computed non-linear transfer rates using the WRT-method, the DIA and the TSA using a zero residual term (right panel). X_{nl}^{BB} denotes the non-linear transfer rate of the broad-band spectrum.

Perturbation test

A critical test of the TSA method is its ability to react on a local perturbation of the frequency spectrum. Such test were carried out by Resio and Perrie (1991) and Young and Van Vledder (1993). In aforementioned studies an artificial dip in the frequency spectrum was made in the high-frequency tail of the spectrum, whereafter the spectrum was quickly evolving to an equilibrium situation. In this study a similar dip (perturbation) was made in the spectrum and the ability of the TSA to react on this perturbation was determined. The initial broad-band spectrum was a JONSWAP spectrum with a peak frequency of f_p=0.2 Hz and a peak enhancement factor of γ=2. At a frequency of 0.35 Hz the energy density was halved. Both the broad-band and the perturbation spectrum are shown in the left panel of Figure 3. The right panel of Figure 3 shows the non-linear transfer rates according to the WRT method for the broad-band spectrum (X_{nl}^{BB}), the perturbed spectrum (X_{nl}), and according to the TSA and DIA method. As can be seen in Figure 3, the TSA method accurately reproduces the WRT method, although it slightly under-estimates the local minima and maxima. The DIA also reacts to this perturbation, but less accurate than the TSA. The results of this perturbation test shows that the TSA is able to react to local perturbations of the frequency spectrum, partly because it retains the same degrees of freedom as the WRT method.

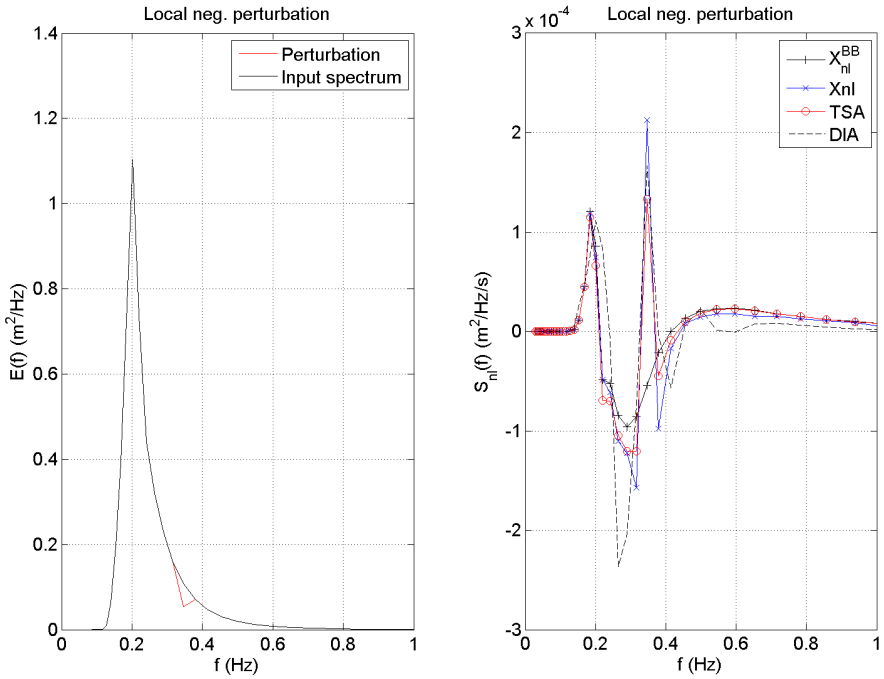

Figure 3: JONSWAP spectrum (black line) with a local perturbation in the high-frequency tail (red line). The right panel shows the exact non-linear transfer rate according to the WRT-method (X_{nl}), the TSA method and the DIA.

Peakedness

As shown by Resio and Perrie (2008) and many others, the non-linear transfer rate is sensitive to the peakedness of the frequency spectrum. Different amounts of peakedness lead to different non-linear responses. This sensitivity is a critical factor in determining

the extent of spectral shapes that needs to be incorporated in the database of pre-computed non-linear transfer rates (broad-band transfer rates) and correction terms (the Λ_d and Λ_p-matrices). It therefore required to assess the amount that an arbitrary spectrum may deviate from the broad-band spectrum before the TSA fails to reproduce the non-linear transfer rate. Therefore, a number of numerical experiments was carried out using a JONSWAP spectrum with a peak enhancement factor of γ=2 as the broad-band spectrum, and a set of arbitrary spectra with peak enhancement factors of γ=1, 1.5, 2.5 and 3. A qualitative analysis suggests that a difference of 0.5 in the peak enhancement factor is still acceptable such that the TSA is able to make a correction to the broad-band transfer rate. It should be noted that a finer resolution of peak enhancement factors in the database yields smaller errors, but it increases the size of the database.

The result of such a sensitivity run is illustrated in Figure 4 showing the performance of the TSA (and DIA) for a JONSWAP spectrum with a peak enhancement of γ=1.5, while using a JONSWAP spectrum with a peak enhancement factor of γ=2 as the broad-band spectrum. The left panel of Figure 4 shows the broad-band spectrum (black line) and the arbitrary spectrum with a peak enhancement factor of γ=1.5 (red line). The right panel shows the result of the WRT, TSA and DIA methods. The results in this figure show that the TSA makes a correction in the right direction only in the frequency range close to the peak frequency, whereas at frequencies higher than, say, 0.3 Hz, the TSA does not correct the transfer rate according to the broad-band spectrum.

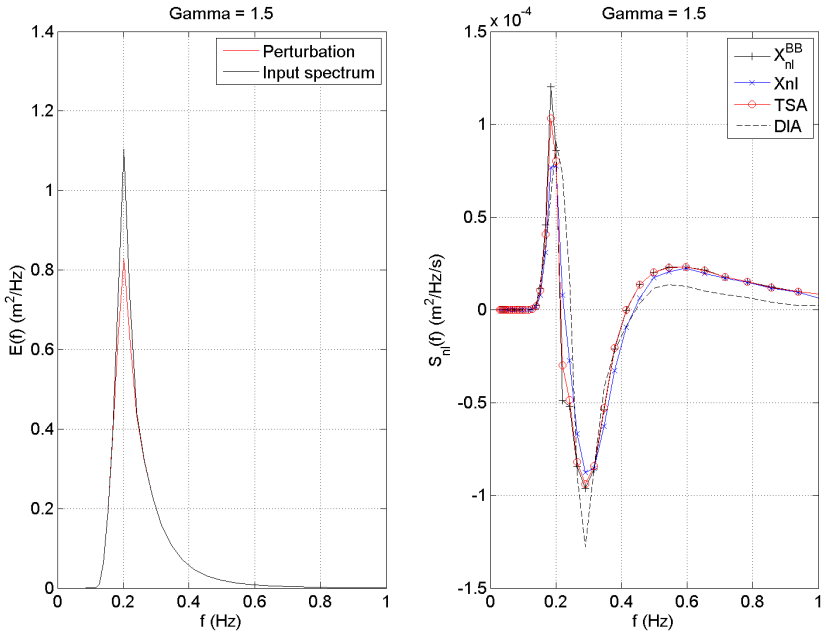

Figure 4: JONSWAP spectra with peak enhancement factors of 2 (broad-band spectrum, black) and 1.5 (arbitrary spectrum, red line) shown in left panel. Non-linear transfer rate according to the WRT method for the broad-band spectrum (X_{nl}^{BB}) and the arbitrary spectrum (X_{nl}), and according to the TSA and DIA methods.

Directional spreading
Similar to the sensitivity of the non-linear transfer rate to the spectral peakedness, the non-linear transfer rate is also sensitive to the amount of directional spreading (cf. Resio and Perrie, 2008). Like the peakedness, the sensitivity to the directional spreading is a critical factor in determining the required number and step size of directional spreading values (using the directional spreading σ of the $\cos^{2s}$-model as the representative parameter) that needs to be incorporated in the database of pre-computed non-linear transfer rates (broad-band transfer rates) and correction terms (the Λ_d and Λ_p-matrices). Here, the directional spreading σ is defined as the circular spreading according to Kuik et al. (1988).

It therefore required to assess the amount of directional spreading that an arbitrary spectrum may deviate from the broad-band spectrum before the TSA fails to reproduce the non-linear transfer rate. A number of numerical experiments was carried out using a JONSWAP spectrum with a peak frequency of 0.2 Hz, a peak enhancement factor of γ=2 and a directional spreading of 30° as the broad-band spectrum, and a set of arbitrary spectra with the same shape of the frequency spectrum but with different amounts of directional spreading, viz: 20°, 25° and 35°. A qualitative analysis suggests that a difference of at most 5° in the amount of directional spreading is still too much for the TSA to make an acceptable correction to the broad-band transfer rate. It should be noted that a finer resolution of directional spreadings in the database yields smaller errors, bit it increases the size of the database. The author realizes that so far no quantitative error measures were used but only qualitative statements differences. A quantitative analysis will be made in further studies.

The result of such a sensitivity run is illustrated in Figure 5 showing the performance of the TSA (and DIA) for a JONSWAP spectrum with a directional spreading of 25°, while using a JONSWAP spectrum with a directional spreading 30° as the broad-band spectrum. The left panel of Figure 5 shows the broad-band frequency spectrum (black line). The right panel shows the result of the WRT, TSA and DIA methods. The results in this figure show that the TSA reacts on the perturbation but fails to make a correction in the right direction. Clearly, a difference of 5° in the amount of directional spreading is too large for the TSA to handle properly, at least in this example.

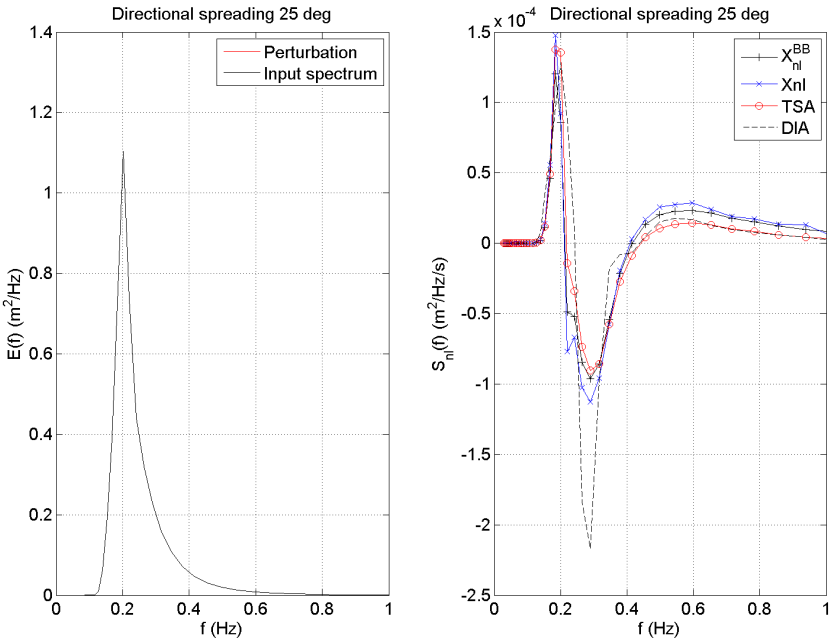

Figure 5: JONSWAP frequency spectrum (left panel). Non-linear transfer rate according to the WRT method for the broad-band spectrum (X_{nl}^{BB}) and the arbitrary spectrum (X_{nl}), and according to the TSA and DIAmethods.

Scaling

Fortunately, scaling rules exist that can be used to transform non-linear transfer rate of similarly shape frequency spectra. It can be shown that for spectra of the form

$$E(f,\theta) = \alpha f_p^{-n} \Psi(\upsilon,\theta) \tag{14}$$

with $\nu=f/f_p$, the nonlinear transfer rate of energy density spectra can be expressed as

$$S_{nl}(f,\theta) = \alpha^3 f_p^{11-3n} \Omega(\upsilon,\theta) \tag{15}$$

In addition, rotational symmetry exists for two similar spectra that only differ in their mean directions. In the case of spectra with two different mean directions $\theta_{m,1}$ and $\theta_{m,2}$, the non-linear transfer rate is rotated over the angle $\Delta\theta=\theta_{m,1}-\theta_{m,2}$. Applying these rules to two similarly shaped spectra, but with different shape parameters α, f_p and θ_m, gives the following relationship valid for JONSWAP type spectra with either an f^{-4} or an f^{-5} spectral tail:

$$S_{nl}^{(2)}(f,\theta) = S_{nl}^{(1)}\left(f\frac{f_{p1}}{f_{p2}}, \theta-\Delta\theta \right)\left(\frac{\alpha_2}{\alpha_1}\right)^3 \left(\frac{f_{p2}}{f_{p1}}\right)^{-4} \tag{16}$$

with $\Delta\theta=\theta_{m,2}-\theta_{m,1}$. The transformation rules and rotational symmetry reduce the number of required pre-computed spectra and related transfer rates and matrices.

An example of the scaling of non-linear transfer rates for two similar spectra but with different scale factors and peak frequencies is shown in Figure 1, although for higher frequencies the scaling is not perfect. This is due to the finite frequency range for which the transfer rate is computed.

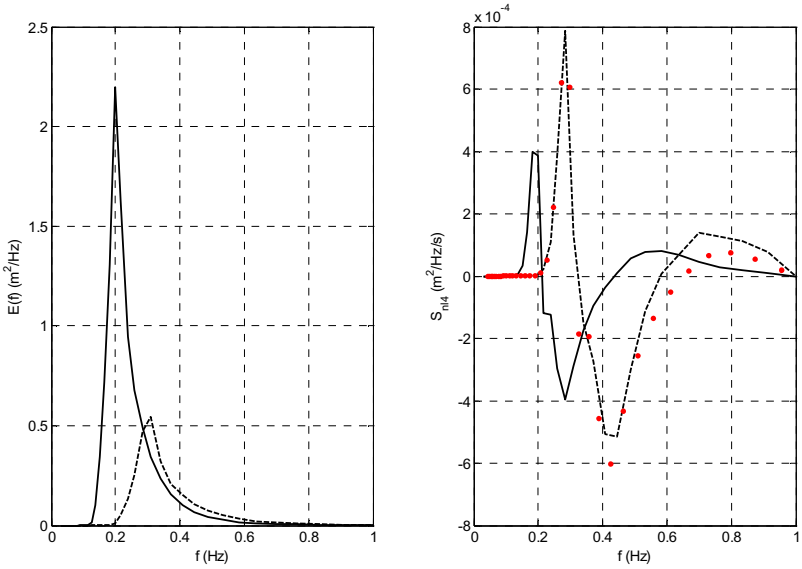

Figure 6: JONSWAP spectra (γ=2) with peak frequencies of 0.2 Hz and 0.3 Hz and related non-linear transfer rate. The scaled transfer rate is indicated by the red dots.

Application of the TSA in a discrete spectral wave model

The basic steps in the TSA subroutine for the computation of the non-linear transfer rate are as follows:

- Determination of the characteristics of the input wave spectrum, viz. the peak frequency f_p, the energy contents E or scale factor α, the mean direction θ, the peakedness γ and the directional spreading σ.
- Search the best corresponding broadband spectrum in the database represented by its peakedness γ, directional spreading σ and for shallow water the dimensionless water depth $k_m h$. In general, this factor will differ from the set of pre-computed peak enhancement values of the broad-band spectra. In such a situation, the nearest discrete value will be taken. This is not a fundamental problem, since the TSA partly corrects for this mismatch. The same argument applies for the other characteristics of the pre-computed broad-band spectra.
- Read the broadband exact non-linear transfer rate and related matrices from file.
- Split the input spectrum into a broadband spectral form and the perturbation term.
- If needed, apply scaling laws and directional transformations to obtain the proper transfer rate for the broadband spectrum and perturbation terms.
- Evaluate TSA correction terms and add these results to obtain the non-linear transfer rate for the transformed arbitrary input spectrum.

The above mentioned steps in the application of the TSA have been addressed in various studies so far. Still, a number of points need further attention before the TSA is generally applicable. These points are the treatment of multi-peaked spectra and the handling of shallow water effects in the computation of the non-linear transfer rate.

Setting up the database
An important feature of the TSA is the use of pre-computed non-linear transfer rates and related matrices for a range of parametric spectra. As noted before their peakedness and directional spreading will characterize these spectra. The sensitivity to variations in the peakedness and directional spreading were explored in this study, although no definite rules could yet be derived. The results suggest that that JONSWAP type peakedness factor can be discretised in steps of 0.5, whereas the directional spreading requires a step less than 5°.

Testing the TSA subroutine
The first step in the development of the TSA was to make a modified version of the WRT method to generate the non-linear transfer rate and related matrices for a given parametric spectrum. This was achieved by making a modified version of the routines developed by Van Vledder (2006). The consistency of this approach was tested in this study.

The second phase of testing the TSA is related to test the scaling of similar spectra. In this phase the following aspects were tested:

- α-scaling for similar spectra but with different energy contents;
- frequency scaling for similar spectra but with different peak frequencies;
- rotational transformation for similar spectra but with different mean directions.

These tests were also carried out successfully.

The third phase is to test the effectiveness of the TSA when the arbitrary input spectra deviates in shape from the parametric spectra for which non-linear transfer rates and related matrices have been computed. Sensitivity tests with spectral shapes deviating from a broad-band spectrum were carried out to get a first impression of the errors that are made by the TSA when the arbitrary spectrum deviates from a broad-band spectrum. In this study, variations in peakedness and directional spreading were applied.

The last and most important phase of the testing is to determine its applicability in operational wave models and its added value compared to the DIA. Academic tests on individual (parametric) spectra are no guarantee that the TSA will also work for spectra that occur during a wave model run. This will involve the following aspects:

- The reproduction of realistic growth curves and their similarity with a wave model version using an exact computation of the non-linear transfer rate, possibly in combination with the retuning of one or more of the other source terms. These tests are needed to show that the system of equations (i.e. the wave action balance equation using the TSA as a subroutine) produces stable results.

- Overall model performance in academic and field cases. Here, model performance is related to integral wave parameters and spectral shapes. Interesting academic cases are the wave model response after a sudden wind shift or a slanting fetch situation. Interesting field cases should be taken from well-documented model studies, e.g. those in Lake George, Australia or at Duck, NC, USA.

5 CONCLUSION

The TSA is a promising technique for the evaluation of the non-linear transfer rate in discrete spectral wave models. It is able to react on a small perturbation of the spectrum. Sensitivity studies indicated that the TSA is able to make corrections to the non-linear transfer of the broad-band spectra and that the scaling technique to compute the transfer rate of similar shaped spectra yields

Further, attention should be given to the ability of the TSA to handle multi-peaked spectra and to have a fast and robust methods to decompose an arbitrary spectrum into broad-band spectra.

Acknowledgements
This work is carried out in the framework of the MORPHOS project of the US Army Corps of Engineers, purchase number W912BU-07-P-0209. Their support and the discussions with Don Resio at USACE, Vicksburg is greatly acknowledged.

References

Hasselmann, K., 1962: On the non-linear energy transfer in a gravity-wave spectrum: Part 1. General theory. J. Fluid Mech., **12**, 481-500.

Hasselmann, S., K. Hasselmann, J.A. Allender, and T.P. Barnett, 1985: Computations and parameterisations of the nonlinear energy transfer in a gravity-wave spectrum. Part 2: parameterisation of the nonlinear transfer for application in wave models. J. Phys. Oceanogr., **15**, 1378-1391.

Kuik, A.J., G.Ph. van Vledder, and L.H. Holthuijsen, 1988: A method for the routine analysis of pitch-and-roll buoy wave data. Journal of Phys. Oceanogr., **18**, 1020-1034.

Long, C.E., and D.T. Resio, 2009: Representation of the Broad-Scale Spectral Form in the Two-Scale Approximation for the Full Boltzmann integral. Proc. 11th Int. Workshop on Wave Hindcasting and Forecasting, 18-23 Oct, Halifax, NS, Canada.

Resio, D.T., and W. Perrie, 1991: A numerical study of nonlinear energy fluxes due to wave-wave interactions. Part 1: Methodology and basic results. J. Fluid Mech., **223**, 609-629.

Resio, D.T., W. Perrie, S. Thurston, and J. Hubertz, 1992: A generic third-generation mave model: AL. Proc. 3rd Int. Workshop on Wave Hindcasting and Forecasting, May 19-22, Montreal, Québec, Canada.

Resio, D.T., and W. Perrie, 2008: A two-scale approximation for efficient representation of nonlinear energy transfers in a wind wave spectrum. Part 1: Theoretical development. J. of Physical Oceanography, 38, No. 12, 2801-2816.

Resio, D.T., and W. Perrie, 2009: A two-scale approximation for efficient representation of nonlinear energy transfers in a wind wave spectrum. Part 2: Application to observed wave spectra. J. of Phys. Oceanography, in press.

Tracy, B.A., and D.T. Resio, 1982: Theory and calculation of the nonlinear energy transfer between sea waves in deep water. WIS Technical Report 11, US Army Engineer Waterways Experiment Station, Vicksburg, Mississippi, USA, 47 pp.

Van Vledder, G.Ph., 2006: The WRT method for the computation of non-linear four-wave interaction in discrete spectral wave model. Coastal Engineering, **53**, 223-242.

Van Vledder. G.Ph., 2007: Operationalisation of the TSA for the computation on no-linear four-wave interactions in discrete spectral wave model. Proc. 10th Int. Workshop on Wave Hindcasting and Forecating and Coastal Hazards. Oahu, Hawaii.

Van Vledder, G.Ph., T.H.C. Herbers, R.E. Jensen, D.T. Resio and B.A. Tracy, 2000: Modelling of non-linear quadruplet wave-wave interactions in operational wave models. Proc. 27th Int. Conf. On Coastal Engineering, Sydney, pp. 797-811.

Webb, D.J., 1978: Non-linear transfers between sea waves, Deep-Sea Res., **25**, 279–298.

Young, I.R, and G.Ph. van Vledder, 1993: A review of the central role of nonlinear interactions in wind-wave evolution. Phil. Trans. R. Soc. London. A, **342**, 505-524.